

Investigation on structural modification of CuInSe₂ solar cell absorber by Al addition

Fianti and Kyoo Ho Kim*

School of Materials Science and Engineering, Yeungnam University, Gyeongsan 712749, Korea

Investigation was performed on chalcopyrite materials of solar cell absorbers, Cu(In,Al)Se₂, to observed the CuInSe₂ structural modification by Al addition. The investigation was done by Cu(In,Al)Se₂ preparation, i.e. pulsed laser deposition and selenization, and characterization, i.e. film composition, structure, and morphology. The Al composition of the films was varied, i.e. 0, 3.8%, 8.2%, 11.3%, 16.6, and 25.6% of [Al]/[In + Al]. The results show that Al can be used for In substitution in CuInSe₂ and keeping the chalcopyrite structure. In tetragonal of Cu(In,Al)Se₂ chalcopyrite, the Al addition modifies the lattice parameter *c*, where the more Al addition to CuInSe₂, the lattice parameter *c* will be shorter, revealing that the Al substitutes In in the parallel line of *c*-axis that causes the compressed tetragonal configuration. By this, the structure of thin film absorber based on CuInSe₂ chalcopyrite can be modified by Al addition for a good solar cell application.

Key words: Structural modification, Cu(In,Al)Se₂, Solar cell.

Introduction

Cu(In,Al)Se₂ is one of chalcopyrite materials which is developed through the addition of Al to CuInSe₂. The Al substitutes a part of In composition which is in the same group of periodic table, group III. Since coming from the same group, Al was designed to keep the chalcopyrite formation with a little modification in the properties, e.g. wider band gap energy from 1.04 eV (CuInSe₂) to 2.67 eV (CuAlSe₂), optically [1] and bigger grain size, morphologically [2].

Cu(In,Al)Se₂ chalcopyrite is identified by using CuInSe₂ and Cu(In,Al)Se₂ because there is no CIAS files of Joint Committee on Powder Diffraction Standards (JCPDS) until now [1, 3-4]. The Al was reported having ability to shift the X-ray diffraction pattern, i.e. the pattern will shift to the greater diffraction angle, 2θ , by the more Al addition in CIAS film [3, 5-11]. Previous reports have calculated the structural properties, such as lattice spacing *d* of 112 plane diffraction, lattice parameter *a* and *c*, tetragonal distortion constant, and cell volume [4-5, 7, 12]. However, the structural investigation has not explained about the Al effect to the modification of Cu(In,Al)Se₂ chalcopyrite tetragonal until now, such as correlation between Al addition and tetragonal deformation also on which side Al substitutes the In at tetragonal configuration. Therefore, this research was carried out on Cu(In,Al)Se₂ chalcopyrite to investigate the CuInSe₂ structural modification by Al addition. This covered the phase formation of Cu(In,Al)Se₂

chalcopyrite and further on how Al modifies the chalcopyrite tetragonal by analyzed the correlation among Al addition, lattice parameter *a* and *c*, tetragonal distortion constant, and cell volume. This investigation will provide a clue about in which side Al substitutes In at tetragonal of the Cu(In,Al)Se₂ chalcopyrite. The film morphology was analyzed to support the structural analysis. By the film morphology, i.e. surface and cross section, the phase formation in thin film could be determined, whether the Cu(In,Al)Se₂ chalcopyrite was formed in single phase or with unwanted secondary phase.

The thin film based on Cu(In,Al)Se₂ chalcopyrite is used for solar cell absorbers. Therefore, this investigation is important because the structure is responsible to the other properties, such as optical and electrical properties which determine the solar cell performance. This investigation was done on Cu(In,Al)Se₂ thin films with varied Al composition ratios, presented by [Al]/[In + Al]. The investigation was done by Cu(In,Al)Se₂ thin film preparation, i.e. Pulsed Laser Deposition (PLD) and selenization, and characterization, i.e. film composition, structure and morphology. The results, discussion, and conclusion were presented in the next sections.

Experiment

Precursor preparation

The precursor films were prepared sequentially by PLD using high purity targets (99.99% purity), i.e. bulk Al, bulk Cu, and powder-compacted In-Se, [In]/[In + Se] = 0.25. The Al, Cu, and In-Se targets were 2.5 cm, 2.5 cm, and 1 cm in diameter and the distance from the Al, Cu, and In-Se target to the substrate were 3.5 cm, 3.5 cm, and 3.8 cm, respectively. A pulsed

*Corresponding author:
Tel : +82-538102475
Fax: +82-538104628
E-mail: khokim@yu.ac.kr

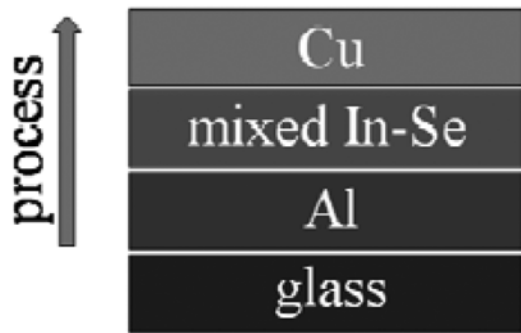


Fig. 1. Three layer deposition of precursor stacking model.

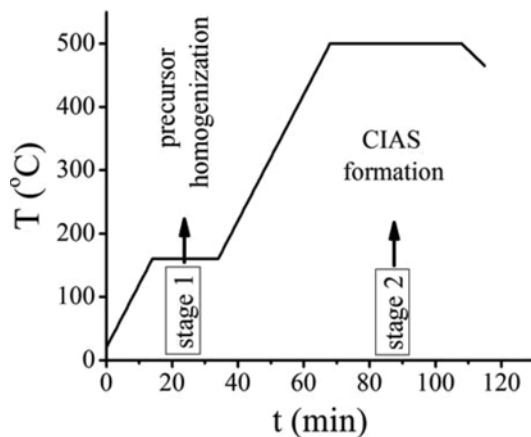


Fig. 2. Heating profile of selenization.

Nd : YAG laser ($\lambda = 1064$ nm) with a 270 μ s laser pulse delay and 0.45 W was used as the deposition source. The working pressure in the PLD chamber was 4.8×10^{-4} Pa.

The precursors were prepared at room temperature using three layer deposition model, as illustrated in Fig. 1. The Al layer was deposited firstly on a glass substrate, then In-Se layer, and finally Cu layer was deposited on the top for capsulation. Al layer was deposited on the glass for film adhesivity to the substrate [13-14] and reducing the possibility of Al_2O_3 formation on the surface caused by an unincorporated Al to $CuInSe_2$ during $Cu(In,Al)Se_2$ formation in selenization [6]. In-Se layer was deposited on the Al layer and under Cu layer to let In-Se binary form prior to $Cu(In,Al)Se_2$ formation and diffuse to the other layers for film homogenization. Finally, Cu layer was deposited on the top to prevent Cu oxidation [14-15], i.e. Cu diffusion to the glass substrate, and reduce In evaporation during selenization. The precursor composition was controlled by adjusting the deposition time.

Selenization

The precursors were placed into an alumina crucible within Se drops (99.99% purity) as selenization source. The crucible was then covered with Al foil to ensure a sufficient Se atmosphere. The selenization process was

run using a programmed heating profile in Ar ambient through two temperature holding steps: 156 °C for 20 min (stage 1) and 500 °C for 40 min (stage 2), Fig. 2. Stage 1 was used to melt the In, allow In diffusion into other layers as liquid state, and then homogenize the precursor. Stage 2 was used to form $Cu(In,Al)Se_2$ according to the conversion of $CuInSe_2$ to $Cu(In,Al)Se_2$ which is initiated at 500 °C [16].

Characterization

The thin film was characterized by IMS-6f Magnetic Sector SIMS, CAMECA, using Cs^+ Gun with impact energy 5 keV and current 50 nA at area (Φ) 30 μ m for the depth profile composition. The thin film was characterized by electron dispersive X-ray spectroscopy, HORIBA, with impact energy 15 keV and working distance 20 cm for the composition ratio. Structural phase analysis was performed by X-ray diffraction PANalytical, using $Cu K_{\alpha}$ radiation ($\lambda = 0.15418$ nm). The film morphology was observed by scanning electron microscopy, SEM-4800 Hitachi.

Result and Discussion

Film composition

The film depth profile show that the film composition is almost constant from the top to the bottom with a little and linear increasing of Al composition in reaching the glass substrate, Fig. 3. This is caused by the stacking model of precursor where Al layer was deposited firstly on the glass substrate. The high Se concentration until 100 nm depth was come from the rich Se in the atmosphere during selenization. The almost constant composition from the top to the bottom reveals that the film is homogeneous which is caused by the precursor stacking model and heating profile in selenization. Each element decreases rapidly after 1300 nm of depth which indicates that the film thickness is 1300 nm, approximately.

All films were designed to have constant Se composition, i.e. $48 \text{ at.}\% < [Se]/[Cu + In + Al + Se] < 51 \text{ at.}\%$ to eliminate the Se effect in the investigation. The metallic composition is in atomic ratio with $[Cu] + [In] + [Al] = 100\%$ and $[Al]/[In + Al]$ from 0 to 25.6%, respectively, Table 1.

Morphology

All cross section images show that $Cu(In,Al)Se_2$

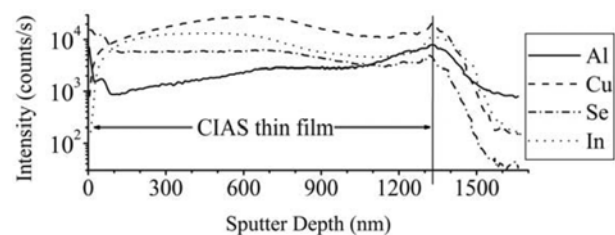


Fig. 3. Depth profile composition of CIAS thin film.

Table 1. CIAS thin film composition.

[Al]/[In + Al] (%)	[Cu] (at.%)	[In] (at.%)	[Al] (at.%)	[Cu]/[In + Al]
0	49.9	50.1	0	1
3.8	39.1	58.6	2.3	0.6
8.2	40.3	54.8	4.9	0.7
11.3	51.2	43.3	5.5	1
16.6	39.3	50.6	10.1	0.6
25.6	36.4	47.3	16.3	0.6

films are adhesive to the glass substrate which are caused by the Al deposition firstly on the substrate, Fig. 4. The surface and cross section morphologies of films with 3.8%, 8.2%, 16.6%, and 25.6% Al addition show uniform grains which are revealing single phase formation of Cu(In,Al)Se_2 chalcopyrite polycrystallines, Fig. 5. Addition, the cross section images of films with 0 and 11.3% Al addition show other particles on the surface which are Cu-Se secondary phases. The film morphologies do not show any significant changing that is caused by Al gradient. The big grains in films with 0 and 11.3% Al addition are caused by the stoichiometric composition, $[\text{Cu}]/[\text{In} + \text{Al}] = 1$, Table 1.

Structure

The XRD patterns show diffraction peaks sequentially at 26.6, 44.2, and 52.4 °2θ which are match with CuInSe_2 files for 112, 204/220, and 116/312 plane which are used to Cu(In,Al)Se_2 chalcopyrite identification, Fig. 5. It shows that In can be substituted by Al for keeping the chalcopyrite structure and Cu(In,Al)Se_2 chalcopyrite can be formed with 0-25.6% Al addition.

X-ray diffraction patterns in Fig. 5 show Cu(In,Al)Se_2 single phase formation at thin films with 3.8%, 8.2%, 16.6%, and 25.6% Al addition and Cu poor composition, $[\text{Cu}]/[\text{In} + \text{Al}] < 1$ (Table 1). In other hand, the Cu(In,Al)Se_2 chalcopyrite phase was formed with Cu-Se secondary phases, i.e. CuSe_2 and Cu_2Se at thin films without Al addition and CuSe_2 at thin films with 11.3% Al addition. The Cu-Se binary phase formation was independent from the Al addition, but was triggered by the stoichiometric composition, Table 1. Therefore, we can conclude that the Cu(In,Al)Se_2 diagram phase is close to the diagram phase of CuInSe_2 system in the sense that CuInSe_2 consists of a two-phase mixture of CuInSe_2 and Cu_2Se at stoichiometry and CuInSe_2 single phase is formed at off-stoichiometry of In rich CuInSe_2 composition which can be seen in phase diagram of $\text{Cu}_2\text{Se-In}_2\text{Se}_3$ pseudobinary section of CuInSe_2 system [17].

The single phase of Cu(In,Al)Se_2 chalcopyrite at off-stoichiometric composition was supported by the defect pair ($2V_{\text{Cu}} + \text{In}_{\text{Cu}}$) development in the chalcopyrite tetragonal that the Cu poor condition led Cu vacancy (V_{Cu}) form with low formation energy [18]. This V_{Cu} was electrically neutralized by antisite defect point of

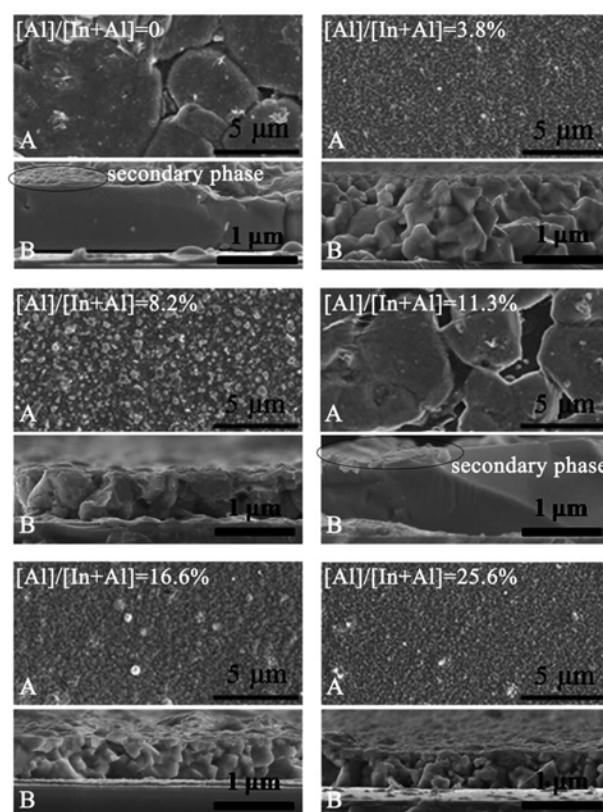


Fig. 4. The surface, A, and cross section, B, morphologies of Cu(In,Al)Se_2 thin films. The Cu-Se secondary phases are located on the surface that can be seen in cross section images of thin films with $[\text{Al}]/[\text{In} + \text{Al}] = 0$ and 11.3%.

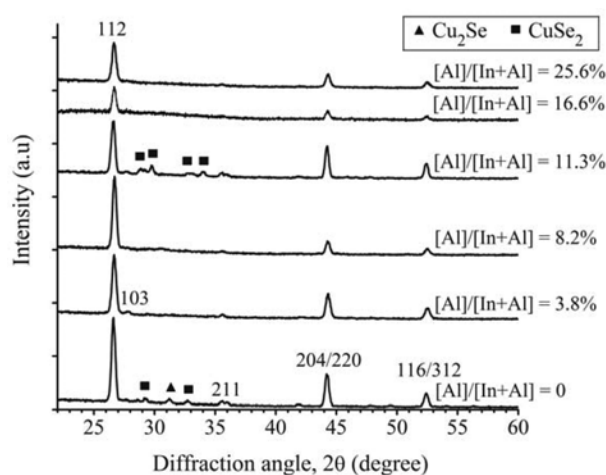
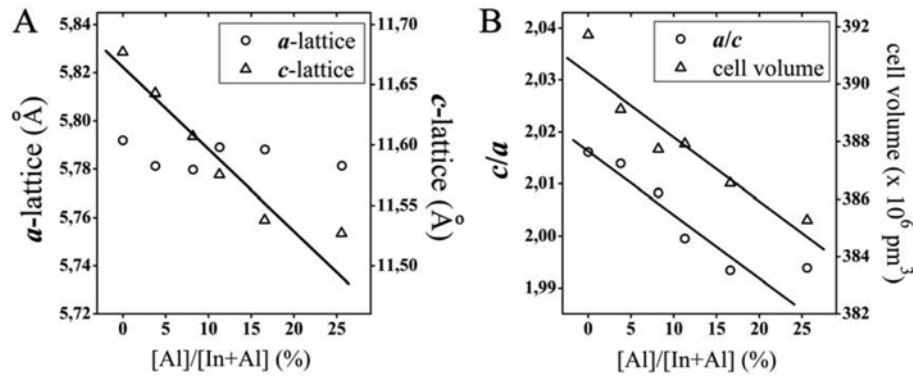


Fig. 5. X-ray diffraction patterns and phase formation of Cu(In,Al)Se_2 thin films with $[\text{Al}]/[\text{In} + \text{Al}] = 0, 3.8\%, 8.2\%, 11.3\%, 16.6\%$, and 25.6% , respectively.

In at Cu site (In_{Cu}). In Cu(In,Al)Se_2 chalcopyrite system with Cu poor condition, the formation energy of Al_{Cu} (antisite defect point of Al at Cu site) shall higher than that of In_{Cu} . This is an analogical interpretation from Cu(In,Ga)Se_2 where the antisite of Ga in Cu site (Ga_{Cu}). defect point has higher formation energy than that of In_{Cu} because the band gap energy of CuGaSe_2 (1.68 eV) is higher than that of CuInSe_2 (1.04 eV) [19].

Table 2. Cu(In,Al)Se₂ chalcopyrite properties calculated according to X-ray diffraction: peak position and lattice spacing d of 112, 204/220, and 116/312.

[Al]/[In + Al] (%)	112 (°2θ)	204/220 (°2θ)	116/312 (°2θ)	d 112 (Å)	d 204/220 (Å)	d 116/312 (Å)
0	26.5850	44.2294	52.4603	3.3529	2.0478	1.7442
3.8	26.6450	44.3158	52.4082	3.3455	2.0440	1.7458
8.2	26.6772	44.3277	52.5042	3.3415	2.0434	1.7428
11.3	26.6728	44.2527	52.4104	3.3420	2.0467	1.7457
16.6	26.7050	44.2600	52.4318	3.3381	2.0464	1.7451
25.6	26.7350	44.3150	52.4519	3.3344	2.0440	1.7445

**Fig. 6.** Graphic of a - and c -lattice versus [Al]/[In + Al], A, and graphic of c/a and cell volume versus [Al]/[In + Al], B, of Cu(In,Al)Se₂ chalcopyrite structure.

So that, the antisite defect point in compensating the composition for Cu(In,Al)Se₂ single phase formation is In_{Cu}, the same phenomenon between CuInSe₂ and Cu(In,Al)Se₂ chalcopyrite system.

The diffraction peak positions for each 112, 204/220, and 116/312 plane of Cu(In,Al)Se₂ chalcopyrite were arranged in Table 2 and transformed into lattice spacings, d , by using Bragg's Equation,

$$n\lambda = 2d\sin\theta. \quad (1)$$

n is an integer, λ is the wavelength of incident wave ($\lambda = 0.15418$ nm), d is the spacing between the planes in the crystal lattice, and θ is the angle between the incident ray and the scattering plane.

Table 2 shows increasing values of 112 diffraction angle in the range of 0.15 °2θ and random changing values of 204/220 °2θ and 116/312 °2θ diffraction angle in the range of 0.0983 °2θ and 0.096 °2θ at increasing of Al addition, 0-25.6%. Those give the same tendencies in lattice spacing, d , where the d_{112} increases 0.0185 Å, in other hand, $d_{204/220}$ and $d_{116/312}$ oscillates in the range of 0.0044 Å and 0.003 Å. To see the structural modification caused by Al addition, the lattice spacing should be transferred into lattice parameter a and c , tetragonal distortion constant (c/a), and cell volume. Since the chalcopyrite cell unit is tetragonal, converting from lattice spacing, d , to lattice parameter a and c should use.

$$1/d^2 = [(h^2 + k^2)/a^2] + [l^2/c^2]. \quad (2)$$

The h , k , and l are Miller indices, d is the lattice spacing, a and c are lattice parameter a and c . The calculated lattice parameter a and c , tetragonal distortion constant (c/a), and cell volume of Cu(In,Al)Se₂ chalcopyrite structure were presented in Fig. 6 for convenient analysis.

Since the Cu(In,Al)Se₂ crystal is derivative structure from CuInSe₂ chalcopyrite, the Cu(In,Al)Se₂ has tetragonal configuration where the perfect tetragonal has $c = 2a$ in their lattice parameters, so that the a -lattice ordinate range (0.125 Å) was designed to be a half of c -lattice ordinate range (0.25 Å) for easier comparison, Fig. 6A. The lattice parameter a shows small fluctuation, random values, and no tendency according to the more Al addition that can be assume as error value revealing that no Al addition effect to the lattice parameter a in tetragonal modification of Cu(In,Al)Se₂ chalcopyrite structure. On other hand, the lattice parameter c shows decreasing value according to the more Al addition that can be assume as clear tendency revealing that Al addition affects the lattice parameter c in tetragonal modification.

Those assumptions were supported by Fig. 6B where the distortion constant and cell volume decrease in the increasing of Al addition. It means that the gradual changing in lattice parameter c is more dominant than that of the lattice parameter a . This can be interpreted that the Al addition affects the lattice parameter c and

does not affect the lattice parameter a . In other words, Al modifies the structure in c -axis of the tetragonal configuration which the more Al addition, the lattice parameter c will be shorter. It means that the Al substitutes In in the parallel line of c -axis, regarding to the smaller Al atom size compared to the In.

The shorter lattice parameter c causes the compressed tetragonal configuration that is responsible to the other properties of Cu(In,Al)Se₂ chalcopyrite, such as optical and electrical properties, where further investigation is required. In structural point of view, we have possibility to design the tetragonal configuration of Cu(In,Al)Se₂ chalcopyrite, one of them, by adjusting the Al addition to CuInSe₂ composition. By this, the thin film absorber based on CuInSe₂ chalcopyrite can be optimized for a good solar cell application.

Conclusions

This research was carried out on Cu(In,Al)Se₂ chalcopyrite to investigate the CuInSe₂ structural modification by Al addition. This covered the phase formation of Cu(In,Al)Se₂ chalcopyrite and further on how Al modifies the chalcopyrite tetragonal. In the phase formation, the results show that Al can be used for In substitution in CuInSe₂ and keeping the chalcopyrite structure which are supported by X-ray diffraction and morphological analysis. Structurally, the Al addition affects the lattice parameter c and does not affect the lattice parameter a , which the more Al addition, the lattice parameter c will be shorter. It means that the Al substitutes In in the parallel line of c -axis and causes the compressed tetragonal configuration of the Cu(In,Al)Se₂ chalcopyrite. Further, the structure of thin film absorber based on CuInSe₂ chalcopyrite can be modified by Al addition that opens possibility to design a good solar cell application.

Acknowledgments

This research was supported by Basic Science Research Program (2013R1A1A2013408) and Center for Inorganic Photovoltaic Materials (No.2012-0001170)

through the National Research Foundation (NRF) grant funded by the Korean government (MSIP).

Reference

1. J.L. Garcia, C. Maffiotte, and C. Guillen, Sol. Energy Mater. Sol. Cells 94 [7] (2010)1263-1269.
2. M. Dhanam, B. Kavitha, and S. Velumani, Mater. Sci. Eng. B 174 [1] (2010) 209-215.
3. S. Yamada, K. Tanaka, T. Minemoto, and H. Takakura, J. Cryst. Growth, 311 [3] (2009)731-734.
4. B. Kavitha and M. Dhanam, J. Ceram. Process. Res. 10 [5] (2009) 652-656.
5. D.C. Perng, J.W. Chen, and C.J. Wu, Sol. Energy Mater. Sol. Cells 95 [1] (2011) 257-260.
6. Y.B.K. Reddy, V.S. Raja, and B. Sreedhar, J. Phys. D: Appl. Phys. 39 [24] (2006) 5124-5132.
7. M. Sugiyama, A. Umezawa, T. Yasuniwa, A. Miyama, H. Nakanishi, and S.F. Chichibu, Thin Solid Films 517 [7] (2009) 2175-2177.
8. A. Umezawa, T. Yasuniwa, A. Miyama, H. Nakanishi, M. Sugiyama, and S.F. Chichibu, Phys. Status Solidi C 6 [5] (2009) 1016-1018.
9. Dhananjay, J. Nagaraju, and S.B. Krupanidhi, Solid State Commun. 127 [3] (2003) 243-246.
10. E. Halgand, J.C. Bernède, S. Marsillac, and J. Kessler, Thin Solid Films, 480-481 [1] (2005) 443-446.
11. D. Prasher and P. Rajaram, Thin Solid Films 519 [19] (2011) 6252-6257.
12. B. Kavitha and M. Dhanam, Superlattices Microstruct. 51 [3] (2012)301-313.
13. K.H. Kim and Fianti, J. Korean Phys. Soc. 60 [12] (2012) 2001-2006.
14. W.A. Lanford, P.J. Ding, W. Wang, S. Hymes, and S.P. Murarka, Thin Solid Films, 262 [1] (1995) 234-241.
15. W. Wang, W.A. Lanford, and S.P. Murarka, Appl. Phys. Lett. 68 [12] (1996) 1622-1624.
16. J. Olejník, C.A. Kamler, S.A. Darveau, C.L. Exstrom, L.E. Slaymaker, A.R. Vandeventer, N.J. Ianno, and R.J. Soukup, Thin Solid Films 519 [16] (2011) 5329-5334.
17. C.H. Chang, A. Davydov, B.J. Stanbery, and T.J. Anderson, in Proceedings of the 25th IEEE Photovoltaic Specialists Conference, Washington, DC, USA, May 1996, (Piscataway, 1996) p.849-852.
18. S.B. Zhang, S.H. Wei, A. Zunger, and H.K. Yoshida, Phys. Rev. B 57 [16] (1998) 9642-9656.
19. S.H. Wei, S.B. Zang, and A. Zunger, Appl. Phys. Lett. 72 [24] (1998) 3199- 3201.